PAPER

Check for updates

Exploring the dielectric properties of HTV silicone rubber based hybrid composites in a multi-stress aging environment

Fateha Aiman,[a] Abraiz Khattak,[e] Arooj Rashid, [ID]*[b] Safi Ullah Butt,[c] Tahira Arshad,[a] Yasin Khan,[d] Khalid Hamad AlKhalid[d] and Abdulrehman Al-Arainy[d]

High temperature vulcanized (HTV) silicone rubber experiences deterioration in electrical performance when subjected to prolonged environmental stresses, limiting its effectiveness in insulation applications. This study investigates the electrical properties of HTV silicone rubber hybrid composites reinforced with nano-silica (2–10%) and micro-ATH (20%) under multi-stress aging for 9000 hours. The results show that hybrid composites exhibit improved electrical performance compared to neat silicone rubber. Notably, the SAT-6 composite displayed the highest DC resistivity (532.57 × 10¹³ Ω m) at 60 °C before aging, with only an 18.5% reduction after aging. SAT-2 demonstrated the smallest increase in the dielectric constant and tan δ, indicating better aging resistance. In contrast, SAT-10 showed the lowest resistivity and the highest increase in dielectric losses due to filler agglomeration and poor dispersion. Overall, leakage current increased after aging, but SAT-6 maintained the lowest value among all aged samples, while SAT-0 showed the highest. These results confirm that the optimal filler loading significantly enhances aging resistance, with up to 6.57% minimal loss in resistivity for SAT-6 at room temperature. These findings show the strong potential of HTV silicone rubber hybrid composites for industrial application in outdoor high-voltage insulation, where improved dielectric stability and long-term durability are critical, enabling reduced maintenance and enhanced reliability in power infrastructure.

1 Introduction

Insulators are crucial components of power and transmission systems as they are used to provide separation between conductors and grounded tower and to provide mechanical support to conductors.[1] Ceramic insulators are widely used as outdoor insulators since they have excellent insulating properties and weather resistance, however, they are heavy, difficult to handle and install, and most importantly they exhibit poor hydrophobicity in polluted and wet environments leading to flashovers.[2] In the last few

decades, researchers and the electric utilities industry shifted their focus towards polymeric insulators and subsequently, their composites due to their advantages over ceramic insulators such as light weight, greater tensile strength, low cost, and superior hydrophobicity, hence excellent pollution performance.[3–9] Silicone rubber based insulators emerged as the favored candidates among the polymeric insulators due to their ability to recover hydrophobicity and transfer low molecular weight (LMW) components from the material bulk to the surface which imparts the hydrophobic characteristics to the pollution layer, hence restraining the flow of leakage current.[10–13] Among the various types of silicone rubbers, vulcanized silicone rubbers are categorized into room temperature vulcanized (RTV), low temperature vulcanized (LTV), and high temperature vulcanized (HTV) types. HTV silicone rubber demonstrated superior properties in outdoor insulation applications.[3] Despite all the advantages of polymeric insulators, achieving long-term performance is still a concern associated with them. Due to their organic nature, environmental stresses such as temperature, ultraviolet (UV) radiation, acid rain, moisture, biological contamination, *etc.* lead to the degradation of polymeric insulators.[14,15] Inorganic fillers are added into base polymers that enhance their resistance to loss of hydrophobicity, partial discharge, erosion and tracking, consequently improving

a United States-Pakistan Center for Advanced Studies in Energy (USPCAS-E), National University of Science and Technology (NUST), Islamabad, 44000, Pakistan. E-mail: fatehaaiman635@gmail.com, abraiz.ktk@gmail.com, tahiraashad544@gmail.com

b Department of Electrical and Computer Engineering (DECE), International Islamic University, Islamabad, 44000, Pakistan. E-mail: arooj.rashid@iiu.edu.pk

c Electrical and Computer Engineering Department, University of Waterloo, 200 University Avenue, Waterloo, ON, N2L 3G1, Canada. E-mail: subutt@uwaterloo.ca

d Department of Electrical Engineering, College of Engineering, King Saud University, Riyadh, Saudi Arabia. E-mail: yasink@ksu.edu.sa, khalkhalid@ksu.edu.sa, aarainy@ksu.edu.sa

e High Voltage Laboratory, GCC Electrical Power Laboratory (GEPL) Company, 3rd Industrial City (MODON-III), Eastern Province, Kingdom of Saudi Arabia

their service life.[16] Most widely used fillers are silica, alumina tri-hydrate (ATH), zinc oxide (ZnO), boron nitride (BN), titania (TiO₂), BaTiO₃, *etc.* Among the insulation characteristics, dielectric properties are crucial as they act as stress relievers for insulation systems.[16] Studies have shown that incorporation of fillers not only improve the weathering performance of composites, but they also improve the insulation characteristics of composites. Farahani *et al.* found that loading silicone rubber with various nano-sized fillers improved the material's dielectric and thermal properties.[17] Zaffer *et al.* found that silicone rubber compositions containing nano Al_2O_3 exhibited superior mechanical, thermal, and dielectric properties.[18] El Hag *et al.* compared nano silica and micro silica filled silicone rubber composites and concluded that nano silica filled composites exhibited significant resistance to erosion in comparison with micro silica filled composites.[19] According to Fang *et al.*,[20] the inclusion of micro-sized SiO_2 and ATH fillers increased mechanical strength and dielectric strength, as well as resistance against tracking and erosion. Deeba *et al.*[21] achieved better and improved dielectric strength with high values of dielectric properties of polymers mixed with different fillers. Faiza *et al.*[22] investigated the dielectric characteristics during aging under various environmental conditions using silicone rubber nano silica and silicone rubber micro silica composites. The results showed that silicone rubber nano silica composites have improved dielectric behavior in comparison with silicone rubber micro silica composites. In another study, dielectric strength and leakage current analyses were performed for 9000 hours on multi-stress aged silicone rubber/ATH/silica micro and hybrid composites. It was assayed that hybrid composites retained their dielectric properties and expressed strong resistance to applied stresses.[23] Nazir *et al.* studied the dielectric response of silica-based micro, nano and hybrid (micro + nano silica) composites of silicone rubber in an intense ultraviolet and thermal environment. It was seen that hybrid composites not only exhibited higher dielectric constant than neat silicone rubber after aging but also expressed lower dielectric loss.[7]

It is evident from the existing literature that fillers significantly enhance the dielectric properties of base polymers. Silicone rubbers, particularly high-temperature vulcanized (HTV) types, are widely used in electrical insulation applications due to their excellent thermal stability and outdoor insulation. This study focuses on exploring the electrical properties of HTV silicone rubber hybrid composites filled with nano-silica and micro-ATH fillers, subjected to 9000 hours of multi-stress aging under conditions involving electrical, thermal, UV, and humidity stresses.

This work also compares the electrical performance of unaged and aged hybrid composites, examining key parameters such as the dielectric constant and dielectric loss concerning temperature and frequency, DC resistivity, AC leakage current, and DC leakage current. For the first time, this study provides a detailed investigation of how nano-silica and micro-ATH fillers influence the long-term electrical stability of HTV silicone rubber under harsh environmental conditions, offering valuable insights for industrial applications requiring durable and reliable insulating materials. A schematic description of the work is given in Fig. 1.

2 Materials and methods

2.1 Materials and sample preparation

HTV silicone rubber was acquired from Dow Corning (USA). Fillers used in this work *i.e.* nano silica (12 nm) and micro-ATH (5 μm) were purchased from Sigma Aldrich (USA). Sample preparation was carried out using the mixing and compounding method. Initially, a suspension of fillers in 100 ml of ethanol was made and stirring was done for 20 minutes followed by ultrasonication for 30 minutes to obtain a uniform suspension. HTV silicone rubber was then introduced into the sonicated mixture. Varox-dicumyl-peroxide was added as a curing agent in the mixture and then mixed for 45 min. The mixture was then transferred into pre-heated steel molds to achieve the desired size and shape of the samples. The mixture
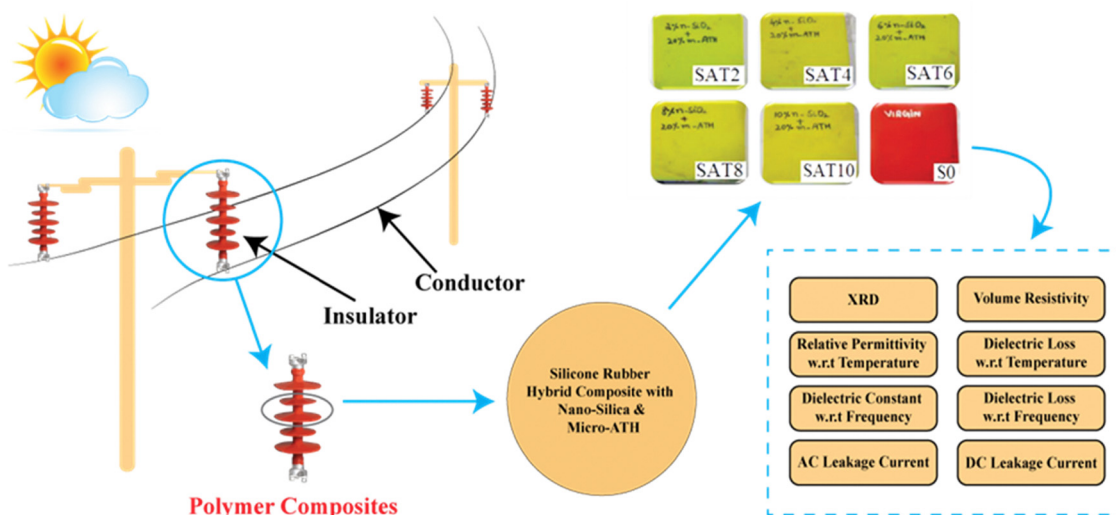

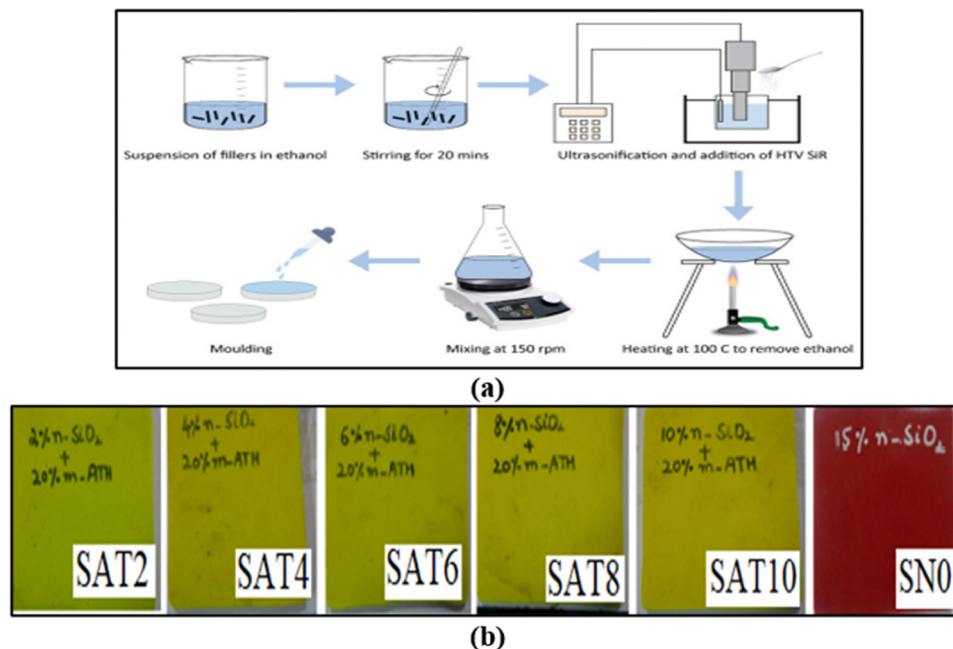Fig. 1 Schematic description of conducted work.

Fig. 2 Sample preparation (a), preparation process (b), and images of the prepared samples.

Table 1 Sample composition description and their codes

	Sample description	
Sample code	Nanosilica wt%	Micro ATH wt%
SAT-2	2	20
SAT-4	4	20
SAT-6	6	20
SAT-8	8	20
SAT-10	10	20
SN0	0	0

was then compressed at 10 MPa and kept at a temperature of 150 °C for 20 min. Finally, the mixture was post-cured at 170 °C for 10 min. The vulcanization reaction is an addition-based curing process, facilitated by the peroxide crosslinking mechanism. The sample preparation process and images of the prepared samples are shown in Fig. 2a and b. In the HTV silicone rubber base material, SiO_2 nanoparticles were incorporated at varying percentages (2%, 4%, 6%, 8%, and 10%), while maintaining a constant ATH percentage of 20%. A neat HTV silicone rubber sample was also prepared for a comparison. Sample description and their respective codes are given in Table 1.

2.2 Aging setup

A 5 ft × 3 ft × 2 ft aging chamber was fabricated to create the intended aging environment. The setup was built according to the EPRI standard.[24] In this special-purpose chamber, the samples were aged simultaneously. The schematic and actual picture of the aging chamber are shown in Fig. 3a and b.

The samples were aged in a multi stress environment for 9000 hours according to summer and winter cycles as described in Table 2 according to the meteorological data of Hattar city, Pakistan. These stresses include electric stress and environmental

stresses like heat, humidity, fog, acid rain, and Ultraviolet (UV) radiation. A 1000 watt heating element was utilized in conjunction with a heat control system for heating. A step-up transformer (220 V/5 kV) was used for providing continuous 2.5 kV to the samples. Three 20 W UV lamps were utilized for a specific number of hours according to daytimes in summers and winters to apply UV radiation.

3 Electrical property analysis techniques

Several measurements and characterization methodologies are used in this research study and will be discussed in detail in the following subsections.

3.1 X-ray diffraction

X-ray diffraction (XRD) operates on the principle of constructive interference of X-rays. In this technique, samples are subjected to incoming X-rays, which interact with the periodic atomic planes in the material. This interaction results in constructive and destructive interferences, producing a diffraction pattern that is recorded for detecting the intensities of the scattered X-rays at specific angles (2θ). The resulting diffraction pattern provides information about the crystal structure, phase composition, and lattice parameters of the material. XRD analysis was conducted using a diffractometer model STOE and Cie from GmbH Germany, operating at 40 kV. The measurement encompassed 2θ values ranging from 10° to 80°, utilizing Cu Kα radiation ($\lambda = 0.15406$ nm) for all the hybrid composites under investigation. XRD measurements were conducted with a peak position uncertainty of $\pm 0.02°$ for 2θ.
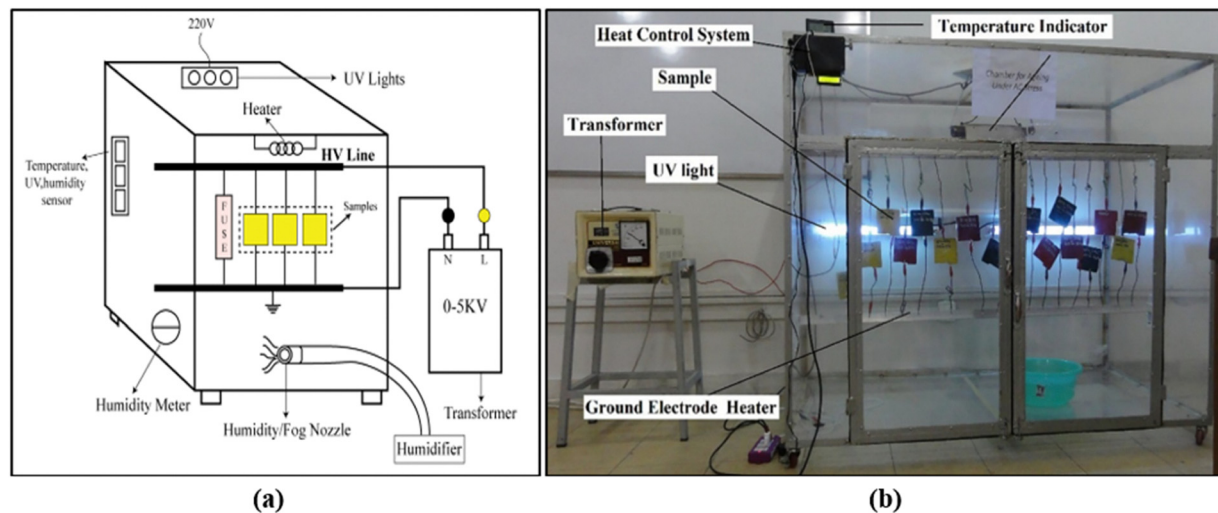
Fig. 3 Multi stressed aging chamber (a), schematic diagram (b) and actual picture.

Table 2 Stress application in summer and winter cycles

Stresses applied	Winter cycle	Summer cycle
No of days	17	11
Ultraviolet radiation/day (1.1 mW cm^{-2})	8 hours	10 hours
Acid rain (4.5 pH)	2 times	6 times
Temperature ($^{\circ}$C)	35.2	47.3
Relative humidity (%)	63	77
Salt fog (6000 μS cm^{-1})	4 times	0 times
Electric stress (kV)	2.5	2.5

3.2 SEM analysis

To investigate surface cracks and roughness of the samples, scanning electron microscopy (SEM) was performed both before and after aging. During SEM analysis, an electron beam was generated and focused on the sample's surface. This beam interacts with the surface and splits into four components: reflected, deflected, absorbed, and stopped electrons. These interactions were detected using various detectors to produce an image. The imaging was conducted under vacuum conditions. A field emission scanning electron microscope (FESEM, Hitachi SU-5000) was utilized for this study.

3.3 DC resistivity

The DC resistivity of a polymer is the capacity to oppose the flow of electric current through a cubic specimen volume. It is entirely reliant on the nature of the material. Temperature, voltage, and the presence of additives impact a polymer's DC resistivity. DC resistivity was measured using Tettex 2830/2831 (Tettex Precision Oil and Solid Dielectric Analyzer) according to ASTM D257/IEC 60093 standard[25] with respective electrode system test cell 2914 at 50 Hz frequency and 2 kV test voltage. DC resistivity was measured with an uncertainty of ±1%, based on the manufacturer's specifications of the Tettex 2830/2831. The DC resistivity values were taken firstly at 28 $^{\circ}$C for all samples and then at 60 $^{\circ}$C.

3.4 Leakage current

Leakage current refers to the electric current that flows through an insulating material indicating some level of conductivity or imperfection in the material. Moisture, surface contamination, impurities, and high temperatures are some of the causes of the flow of leakage current.

3.4.1 AC leakage current. According to IEC 60815 and the creepage distance of the samples, a 2.5 kV supply voltage was selected. A 2.5 kV AC voltage source is connected in series with a 1 kΩ resistor and the sample, as illustrated in Fig. 4. To determine the AC LC, a multimeter is employed to measure the voltage drop across the sample, and the AC leakage current is evaluated using Ohm's law.

$$I = \frac{V}{R} \tag{1}$$

3.5 Dielectric constant and tan δ with respect to temperature

The dielectric constant of a material quantifies its capacity to store electrical energy and indicates how effectively the material can retain or concentrate electric flux. Mathematically, the ratio between the permittivity of a material (ε_m) and permittivity of free space (ε_0) is termed as the dielectric constant.

$$\varepsilon_r = \frac{\varepsilon_m}{\varepsilon_0} \tag{2}$$

A low dielectric constant is desirable for effective electrical insulation. The dissipation factor characterizes the losses that
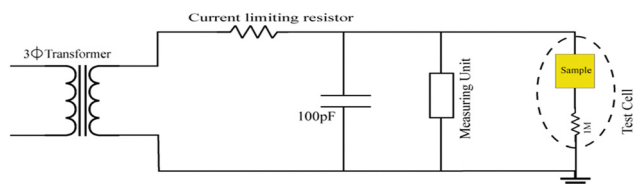

Fig. 4 Setup for measurement of AC leakage current.

take place within insulators. Such losses are in direct proportion with power that gets transferred into heat due to the electric field. Dielectric constant and $\tan\delta$ with respect to temperature were measured using Tettex 2830/2831 (Tettex Precision Oil and Solid Dielectric Analyzer) by IEC 60250[26] with a respective electrode system test cell 2914 at 50 Hz frequency, 2 kV test voltage and temperature from 28 °C to 60 °C. The dielectric constant was measured with an accuracy of ±0.5%, while $\tan\delta$ had a maximum error of ±0.02 over the tested frequency and temperature ranges.

3.6 Dielectric constant and $\tan\delta$ with respect to frequency

The dissipation factor and dielectric constant with respect to frequency were measured using the IET Labs USA 7600 Plus LCR Meter. For measuring the dielectric constant with respect to frequency the uncertainty is ±0.0005. The materials were placed inside the LD-3 inelastic dielectric cell for the measurements. To ensure optimal fit in the dielectric cell, all the samples should have a 60 mm diameter. The measuring frequency range was set at 10 Hz to 2 MHz.

4 Results and discussion

4.1 Confirmation of composites

X-ray diffraction is a method for studying the crystalline structure of materials. The effective inclusion of nano silica and micro-ATH into the polymeric matrix was confirmed by X-ray diffraction. The pattern of micro-ATH particles is classified as a pure monoclinic phase, which is quite close to the values reported in the literature and the definite peak at $2\theta = 18.14°$ indicates that micro-ATH particles are crystallized. Another peak was found at $2\theta = 21.89°$ indicating the presene of nano silica[27] as presented in Fig. 5.

4.2 SEM analysis

The primary objective of SEM analysis was to evaluate the effects of aging on the surface morphology of the samples. Aging in the HTV silicone rubber hybrid composites resulted in increased roughness, material loss, cluster formation, and raised surfaces as depicted in Fig. 6. The more the surface roughness the lower the DC resistivity and *vice versa*. SAT-0 had the smoothest surface before aging but after aging it showed loss of material on the surface.

4.3 DC resistivity

DC resistivity, also known as volume resistivity, is the resistance of a material to the flow of electric current across its volume. It assesses how effectively a material can withstand the flow of electrical current with an applied electric field across its volume. DC resistivity of unaged and aged samples at 28 °C is illustrated in Fig. 7. It is clear from Fig. 7 that the DC resistivity of HTV silicone rubber hybrid composites increased with an increase of nano-silica content up to 8%. A similar trend was observed after accelerated aging. Therefore, the highest DC resistivity was exhibited by the SAT-8 sample, whereas the
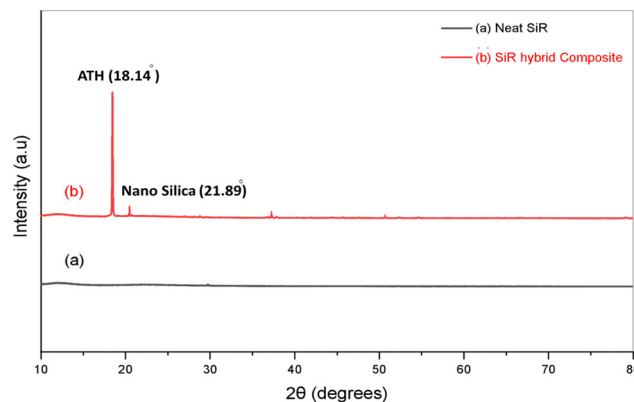

Fig. 5 XRD pattern of (a) neat HTV silicone rubber and (b) silicone rubber hybrid composite.

SAT-10 sample showed the lowest. After aging, the lowest value of DC resistivity was exhibited by the SAT10 sample (240.63 × 10^{13} Ohm m). The minimum loss in percentage was found for the SAT-6 sample after aging (6.57%) as shown in Fig. 7. Overall, all the HTV silicone rubber hybrid composites had higher volume resistance than the SAT-0 sample before and after aging.

Furthermore, the DC resistivities of all samples were measured at 60 °C. Fig. 8 represents that the DC resistivity of unaged and aged neat silicone rubber and silicone rubber hybrid composites showed decreasing behavior as the temperature was increased from 28 °C to 60 °C. This is because higher temperatures lead to increased thermal motion of atoms and electrons within the material. This increased thermal motion can result in more charge carriers becoming available for conduction, thus reducing the material's resistance to electrical current flow. The highest DC resistivity was shown by SAT-6 in comparison to neat HTV silicone rubber and all other hybrid samples before and after aging. In addition to that SAT-6 has a minimum loss percentage (18.5%) after aging for 9000 h. SAT-10 showed adverse behavior in terms of DC resistivity since it showed the lowest resistivity both before and after aging.

The increase in DC resistivity in HTV silicone rubber hybrid composites observed may be because of the dissociation of chains of the polymer by the incorporation of silica particles. The behavior was more prominent for higher nano silica percentages. The increase in DC resistivity values noticed may be due to better intercalation for a certain percentage of the nanofiller and poor intercalation for a higher percentage of nano silica. The poor intercalation may cause the reduction of DC resistivity. SAT-0 had the lowest DC resistivity as compared to all HTV silicone rubber hybrid composites except SAT-10. The main reason may be that when the percentage of nano silica has increased to a certain limit, it has poor intercalation in the base silicone rubber matrix. These results are also supported by the SEM analysis.

4.4 Leakage current

The AC leakage current of unaged and aged samples is shown in Fig. 9. The sample SAT-0 has a higher leakage current in comparison with silicone rubber hybrid composite samples prepared using silica and ATH fillers. A decrease in leakage
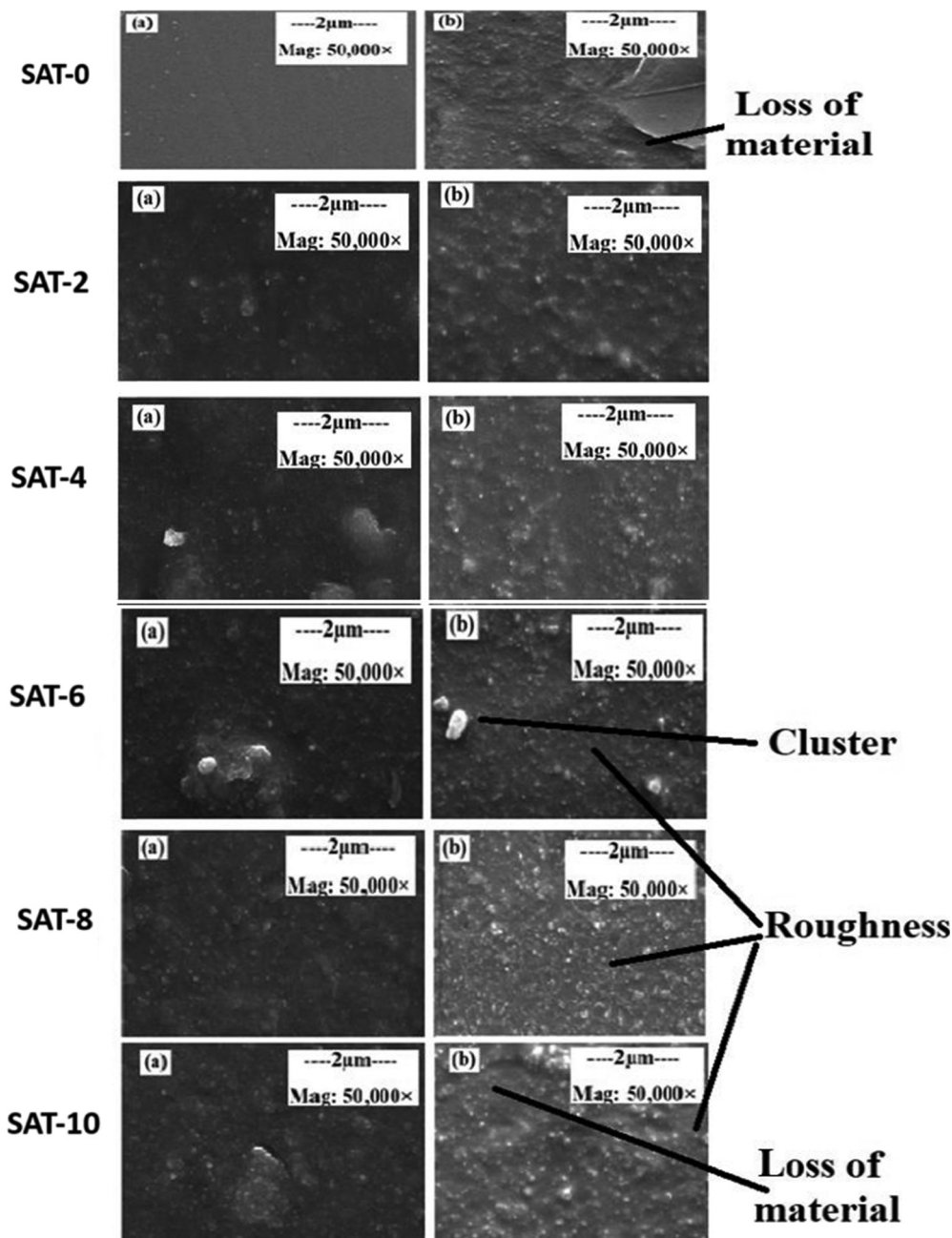
Fig. 6 SEM images: (a) before aging and (b) after aging.

current with the addition of nano silica and micro-ATH can be observed in Fig. 8. The improved overall resistance of silica and ATH may have contributed to the decrease in leakage current in composites. Lower hydrophobicity increases surface resistance, lowering leakage current. SAT-2 showed maximum AC leakage current while SAT-6 showed minimum AC leakage current before aging. Furthermore, the experimental results show an increase in leakage current of neat HTV silicone rubber and silicone rubber hybrid composites after aging as demonstrated in Fig. 9.

SAT-6 shows the lowest value of AC leakage current, whereas SAT-0 shows the highest AC leakage current amongst all aged samples. UV radiation and temperature may be important

contributors to the breakage of $Si-CH_3$ and C–H bonds of silicone rubber. The SAT-6 performed well after aging because very little deterioration was observed. This is because the nanoparticles are at their optimal concentration in the base matrix. The values of AC leakage current for all unaged and aged samples are within the acceptable range of leakage current according to the IEC 60601-1 standard.[28]

4.5 Dielectric constant with respect to temperature

The dielectric constant with respect to temperature of unaged neat HTV silicone rubber and silicone rubber hybrid composites is depicted in Fig. 10.
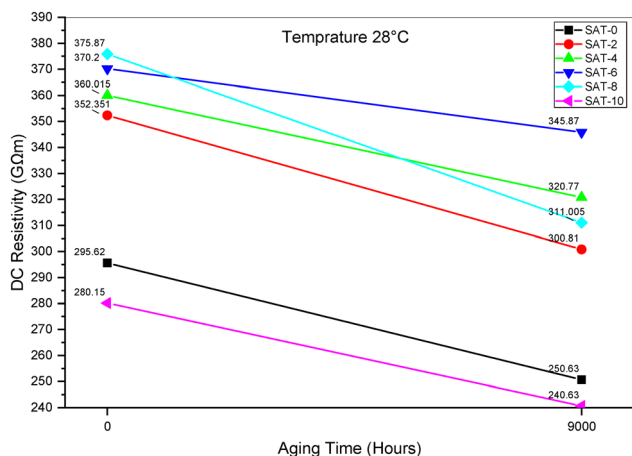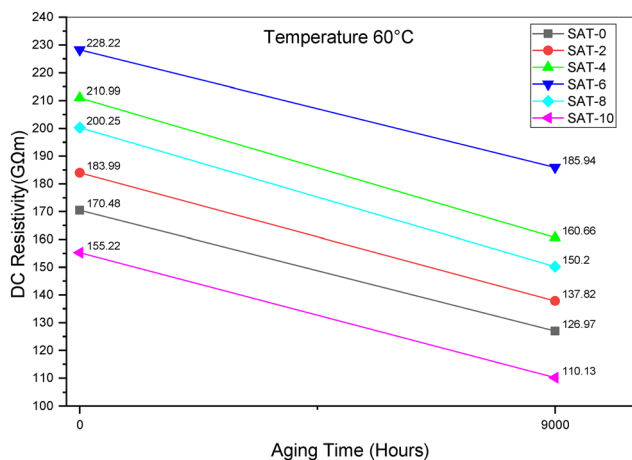
Fig. 7 DC resistivity at 28 °C.

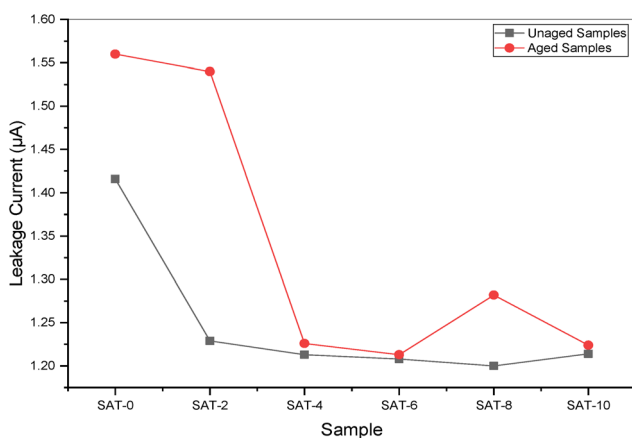**Fig. 8** DC resistivity at 60 °C.

Fig. 9 AC leakage current of unaged and aged samples at 2.5 kV AC.

4.5.1 Dependence of the dielectric constant on the filler concentrations. The amount of filler loading, the size of the filler, the shape of the filler, and the interfacial properties of the composites all have an impact on the dielectric properties of composites.[16] At 25 °C, the dielectric constant of nano silica is roughly 5.72, while that of silicon rubber is 3.3 and that of micro-ATH is 2.2.[17] It is witnessed from Fig. 10 that increasing the concentration of nano silica causes an increase in the value of the dielectric constant of silicone rubber hybrid composites since it has a higher dielectric constant than silicone rubber. ATH on the other hand has a lower dielectric constant than silicone rubber so it does not have any significant effect on the overall dielectric constant of hybrid composites. The increase in the dielectric constant of composite materials is often due to an increase in the filler as reported in the literature.[29] Hence SAT-2 showed the least dielectric constant of all the hybrid composites whereas SAT-10 showed the maximum value of the dielectric constant.

4.5.2 Dependence of the dielectric constant on temperature. The change in the dielectric constant is relatively low with temperature as shown in Fig. 10 for silicone rubber hybrid composites. The relative permittivity of composites decreases with increase in temperature. The relative permittivity of composites decreases with increase in temperature. The large difference in the coefficient of thermal expansion (CTE) between the polymer matrix and filler interrupts the accumulation of polar components and causes a reduction in the dielectric constant with an increase in temperature. Other studies have also proven a decrease in relative permittivity with increasing temperature.[30]

The dielectric constant of all aged samples with respect to temperature is represented in Fig. 11. The dielectric constant of all samples with respect to temperature increased after aging for 9000 h. The reason for this increase may be that when subjected to external stresses, HTV silicone rubber experiences breakages in its polymer chains, affecting both the main and side chains. These fractures disrupt the polymer network, introducing defects and disorders that reduce crystallinity.[31–33] These defects lead to free volume, and spaces between polymer chains, allowing increased molecular motion including bond vibrations and rotations. This enhanced molecular motion boosts polarization, particularly of polarized Si–O bonds, due to the material's disordered state. The fractures make it easier for these polar bonds to realign under an electric field, affecting the relative permittivity of the material. With greater disorder, expanded free volume, and enhanced polarization, the relative permittivity increases. It is clear from Fig. 9 and 10 that after 9000 hours of aging, the dielectric constant of SAT-0 significantly increased. In contrast, the increase in the dielectric constant for the hybrid samples after aging was less compared to their unaged counterparts. Notably, among all the hybrid samples, SAT-2 displayed the lowest dielectric constant both before and after aging.

4.6 tan δ with respect to temperature

The parameter that measures the losses in insulation materials is known as dissipation factor or tan δ.

4.6.1 Dependence of tan δ on filler concentrations. It is evident from Fig. 12 that tan δ increases with increasing
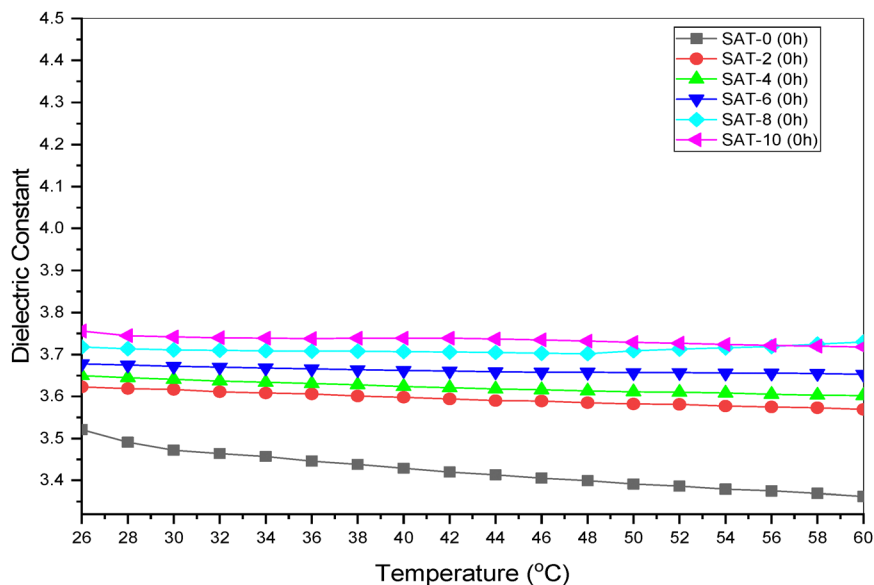
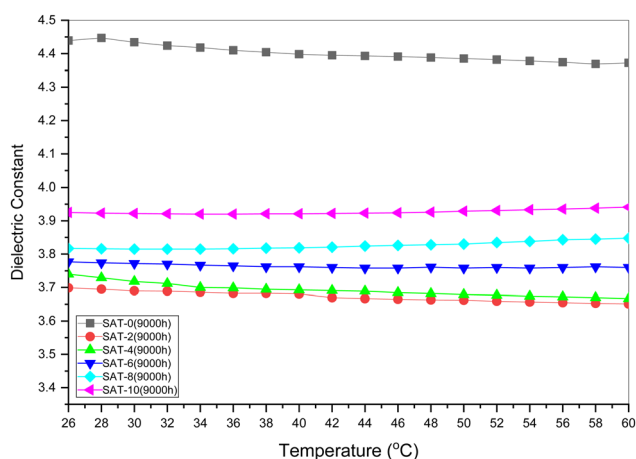Fig. 10 Dielectric constant of unaged samples (Varying Temperature).
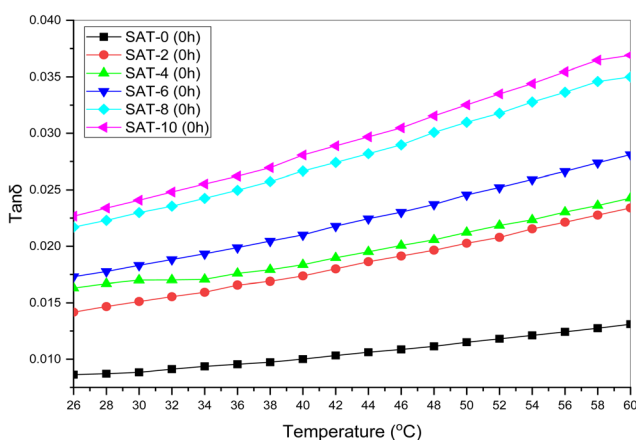

Fig. 11 Dielectric constant of aged samples.


Fig. 12 tan δ of the unaged samples.

filler content. SAT-0 showed a minimum value of tan δ. SAT-10 showed a maximum value of tan δ among all the hybrid samples. This increase in tan δ is attributed to interfacial polarization. Interfacial polarization occurs due to the polymer matrix and filler having a difference in the electrical properties. This polarization produces charge alignment at the interface during cyclic material deformation, resulting in energy loss in the form of heat. Such a result is more prominent as the filler content increases, leading to a higher tan δ value.

4.6.2 Dependence of tan δ on temperature. The value of tan δ increases with the increase in temperature as shown in Fig. 12. All the samples including neat HTV silicone rubber and silicone rubber hybrid composites showed an increasing trend in tan δ with an increase in temperature. This may be because of the increase in the segmental movement of chains of the polymer as temperature increases. This increased mobility allows polymer chains to move more freely, leading to greater energy dissipation and thus a higher tan δ. Additionally, at elevated temperatures, there is an increase in ionic conductivity within the material. This could be due to the enhanced movement of ions, possibly arising from ion dissociation. The movement of ions contributes to energy dissipation and higher loss tangent values.[20]

The tan δ values of neat HTV silicone rubber and all hybrid samples increased after aging as represented in Fig. 13. The dielectric loss of HTV silicone rubber may increase with aging due to a combination of factors, including changes in cross-linking, thermal degradation, oxidation, moisture absorption, alterations in siloxane structures, and mechanical stress. These factors affect molecular mobility, polarization, and relaxation behavior, collectively leading to higher dielectric loss. From Fig. 12 and 13, it is evident that the dielectric loss of SAT-0 significantly increased after aging. Among all hybrid samples, dielectric loss increased after 9000 hours of aging. Notably, SAT-2 displayed

Fig. 13 tan δ of the aged samples.

Fig. 14 Dielectric constant of unaged samples (Varing Frequency).
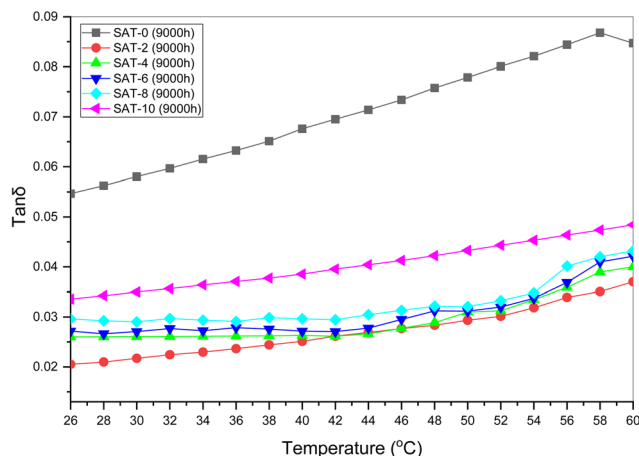
the smallest increase in dielectric loss, while SAT-10 exhibited the most substantial increase.

4.7 Dielectric constant with respect to frequency

The dielectric constants with respect to frequency of virgin HTV silicone rubber and silicone rubber hybrid composites were measured for unaged and aged samples.

4.7.1 Dependence of dielectric constant on frequency. At low frequencies, HTV silicone rubber has a large dielectric constant, but with the increase in frequency, the dielectric constant decreases until it becomes constant. This may be due to the electric charge arrangement in one direction, which reduces with frequency increase. Because polar groups in virgin HTV silicone rubber and its many forms align with the applied electric field, the dielectric constant increases. Because of the increase in frequency, the dipoles are unable to align along their parallel axes to the applied AC field. As a result, when frequency increases, the dielectric constant decreases.

4.7.2 Dependence of the dielectric constant on the filler concentrations. The lowest dielectric constant occurs at 2% nano silica and with increasing concentration of nano-silica in HTV silicone rubber, the dielectric constant of hybrid composite increases as illustrated in Fig. 14. Since the dielectric constant of nano-silica is higher than that of neat HTV silicone rubber, the filler may increase the dielectric constant of the overall composite.

It is demonstrated in Fig. 14 that an increase in the amount of filler resulted in an increase in the dielectric constant which may be due to the formation of aggregates/clusters which is represented in Fig. 15.

The thin immobile nanolayers that surround the nanoparticles offer a stronger contact between the nanoparticles and the second layer of weakly connected polymer at low nanofiller loadings, as seen in Fig. 16. As a consequence, the mobility of chains in the hybrid composite is greatly reduced. When these two processes occur simultaneously with a 2% nano-filler loading, the hybrid composite permittivity will be lowered to the greatest extent at all frequencies. The lowest
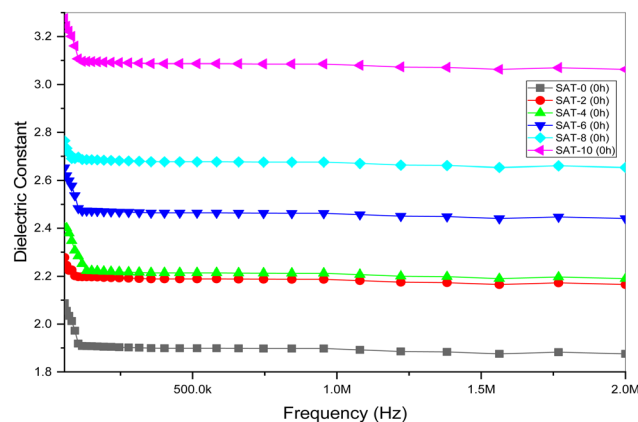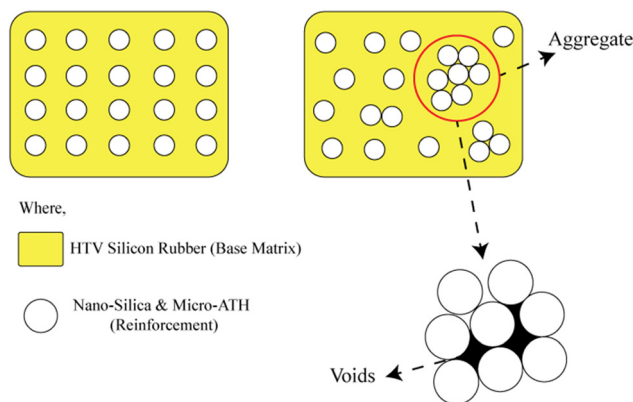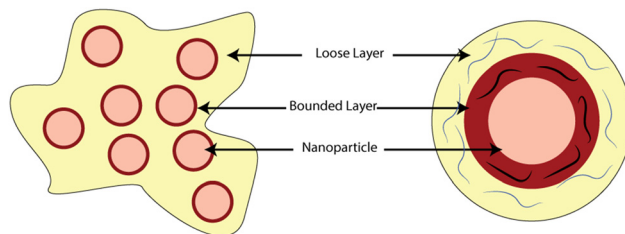

Fig. 15 Formation of aggregates.

Fig. 16 Two layers of nanoparticles.

dielectric constant, as observed at 2% nano-silica concentration, is most likely owing to this.

The dielectric constant of aged samples subjected to various stresses is shown in Fig. 17. It was revealed that the dielectric constant values for the aged samples were greater than those for unaged samples. The same decreasing trend of the dielectric constant with increasing frequency was observed for the unaged and aged neat HTV silicone rubber and silicone rubber hybrid composites. This increase could be attributed to the weakening of grain boundaries. The value of the dielectric constant for SAT-0 in aged samples was 4.05, and it remained above 3.9 for all frequencies. The highest value of dielectric constant 4.19 was shown by SAT-10 amongst all aged samples,
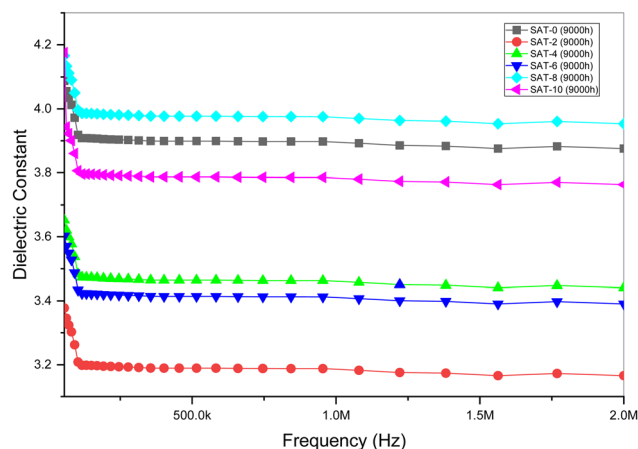
Fig. 17 Dielectric constant of the aged samples.
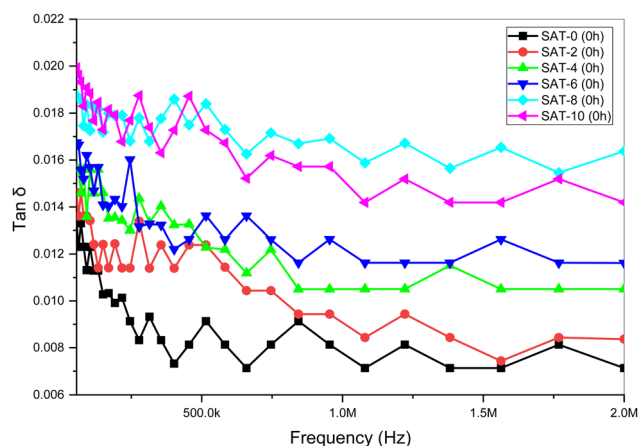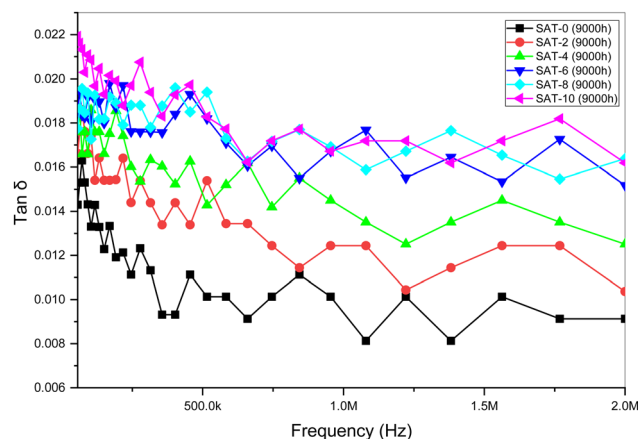

Fig. 19 tan δ of the aged samples.

and it remained over 3.8 for all values of frequencies. The dielectric constant of neat HTV silicone rubber is higher because the polar groups align with the provided electric field. SAT-8 showed a relatively lower value of 4.15 that remained above 3.98. SAT-6 showed a lesser value of 3.67 and showed a constant value above 3.39. SAT-4 exhibited a value of 3.6 that became constant at 3.42. SAT-2 showed the lowest dielectric constant in comparison to all hybrid composites over all frequency ranges. It has a dielectric constant of 3.39 at lower frequencies but it became a constant value of 3.2 at higher frequencies.

4.8 tan δ with respect to frequency

The tan δ value was evaluated in terms of frequency of both neat HTV silicone rubber and silicone rubber hybrid composites with varying amounts of nano silica fillers before and after aging.

4.8.1 Dependence of tan δ on frequency. It is shown in Fig. 18 that tan δ decreases quickly with frequency, exhibiting dispersion at lower frequencies, and then becomes constant at higher frequencies.

4.8.2 Dependence of tan δ on the filler concentrations. The addition of nano silica and micro-ATH increased the tan δ

values, suggesting enhanced charge carrier sources as shown in Fig. 18. Hindrances in charge transport, caused by interface dynamics and polymer chain entanglements, are likely to inhibit charge carrier motion in hybrid composites with low filler loadings. Furthermore, strong bonding between polymer chains and nanoparticle surfaces can yield fewer defects and free charge carriers, lowering electrical conductivity in hybrid composites even further. SAT-10 showed tan δ values that are greater than for both neat silicone rubber and composites with low filler levels. This is likely due to the increased electrical conductivity resulting from a higher number of nanoparticles at this concentration. A greater number of nanoparticles and potential contact between nanoparticles enhance the chances of charge transfer, particularly among lighter electronic species. Additionally, the higher filler concentration leads to more free charge carriers in the system. At 10% filler loading, the overlapping interfacial zones of the nanocomposite enhance charge carrier percolation and increase electrical conductivity overall. The amount of overlap is determined by the distribution of nanoparticles and their size within the silicone rubber matrix. Agglomerations in the nanocomposite can lead to localized charge transport, and the size of nanoparticles dictates the filler loading level at which such overlapping occurs.

It is evident from Fig. 19 that with aging it is observed that the tan δ increases for unfilled HTV silicone rubber as well as silicone rubber hybrid composites. This may be due to the increase in loss caused by the degradation of the samples under the applied electrical and environmental stresses. It has also been observed that the increase in tan δ for silicone rubber hybrid composites after aging is slightly lower than that for the neat HTV silicone rubber.

5 Conclusion

This study investigates the electric properties of silicone rubber hybrid composites subjected to aging under various environmental stresses, revealing valuable insights into their performance and long-term stability. The results demonstrate that SAT-6 exhibited the highest DC resistivity and the lowest

Fig. 18 tan δ of the unaged samples.

percentage loss of resistivity after aging, highlighting its excellent electrical stability. SAT-2, with 2% nano-SiO$_2$ and 20% ATH, consistently displayed the lowest AC and DC leakage currents, both before and after aging, emphasizing its superior performance in maintaining low leakage currents over prolonged periods. Additionally, the hybrid composites showed remarkable resilience to abrupt increases in the dielectric constant and dielectric loss after aging, which underscores their potential for stable performance even under environmental stress.

Under 9000 hours of environmental exposure, SAT-2 maintained the lowest dielectric constant and dielectric loss values across varying temperatures and frequencies. This indicates that SAT-2 is the most stable composite among the samples, making it the ideal option for applications requiring high electrical stability over extended periods. The results of this study suggest that the inclusion of nano-SiO$_2$ with 20% ATH in the composites significantly improved their dielectric properties, contributing to their enhanced stability and performance under aging conditions.

This work advances the existing literature by demonstrating the superior performance of hybrid silicone rubber composites under aging conditions that replicate real-world stresses, particularly in high-voltage insulation systems and outdoor electrical equipment. This study not only highlights the benefits of incorporating nano-SiO$_2$ with 20% ATH but also bridges the gap between material design and practical applications, offering new insights that can be transferred directly to industries focused on durable, high-performance materials. Furthermore, this study emphasizes the importance of hybrid composites in maintaining stable dielectric properties over long periods, an aspect that previous studies have not thoroughly addressed.

However, several challenges remain. The study does not explore the effects of extreme environmental conditions such as high humidity or UV exposure, which may influence a material's long-term performance. Future research should focus on optimizing the composite formulations by experimenting with different filler types or varying the nano-SiO$_2$ content to further enhance the mechanical and electrical properties. Moreover, evaluating the performance of these composites under more aggressive aging conditions and in real-world industrial applications will be crucial for determining their suitability for commercial use. Understanding the full range of environmental effects on these composites will enable the development of materials with even better long-term durability and reliability.

Author contributions

Dr Abraiz Khattak and Dr Yasin Khan: conceptualization, supervision, and project administration. Fateha Aiman: investigation, methodology, roles/writing – original draft, writing – review and editing, data collection, and analysis. Arooj Rashid and Khaled Alkhaled: methodology, validation, and writing – review and editing. Tahira Arshad and A. A. Alrainy: writing – review and editing.

Data availability

Data are available from the authors upon reasonable request. All datasets generated and/or analyzed during the current study are already incorporated in the research paper in the form of graphs and tables. Additional materials such as raw data or detailed data are available upon request from the corresponding author.

Conflicts of interest

The authors declare that there is no conflict of interest.

Acknowledgements

References

1 A. A. Salem, R. Abd-Rahman, S. A. Al-Gailani, M. S. Kamarudin, H. Ahmad and Z. Salam, The leakage current components as a diagnostic tool to estimate contamination level on high voltage insulators, *IEEE Access*, 2020, **8**, 92514–92528.

2 J. E. Contreras and E. A. Rodriguez, Nanostructured insulators–A review of nanotechnology concepts for outdoor ceramic insulators, *Ceram. Int.*, 2017, **43**(12), 8545–8550.

3 M. Akbar, R. Ullah and S. Alam, Aging of silicone rubber-based composite insulators under multi-stressed conditions: an overview, *Mater. Res. Express*, 2019, **6**(10), 102003.

4 M. Amin, A. Khattak and M. Ali, Accelerated aging investigation of silicone rubber/silica composites for coating of high-voltage insulators, *Electr. Eng.*, 2018, **100**(1), 217–230, DOI: **10.1007/s00202-016-0498-7**.

5 N. C. Mavrikakis, P. N. Mikropoulos and K. Siderakis, Evaluation of field-ageing effects on insulating materials of composite suspension insulators, *IEEE Trans. Dielectr. Electr. Insul.*, 2017, **24**(1), 490–498, DOI: **10.1109/TDEI. 2016.006077**.

6 M. T. Nazir, B. Phung, S. Yu and S. Li, Effects of thermal properties on tracking and erosion resistance of micro-ATH/AlN/BN filled silicone rubber composites, *IEEE Trans. Dielectr. Electr. Insul.*, 2018, **25**(6), 2076–2085.

7 M. T. Nazir and B. T. Phung, Accelerated ultraviolet weathering investigation on micro-/nano-SiO2 filled silicone rubber composites, *High voltage*, 2018, **3**(4), 295–302.

8 M. T. Nazir, B. T. Phung, S. Yu, Y. Zhang and S. Li, Tracking, erosion and thermal distribution of micro-AlN+ nano-SiO2 co-filled silicone rubber for high-voltage outdoor insulation, *High Voltage*, 2018, **3**(4), 289–294.

9 S. U. Butt, *et al.*, Investigation of epoxy composites for outdoor insulation under accelerated ultraviolet exposure, *Mater. Res. Express*, 2021, **8**(8), 085303.

10 K. Abraiz, A. Muhammad, A. Muhammad and I. Muhammad, Hydrophobicity investigation and life estimation of silicone rubber nanocomposites, *Emerging Mater. Res.*, 2020, **9**(1), 200–205, DOI: **10.1680/jemmr.17.00055**.

11 Faiza, *et al.*, Investigation of Hydrothermally Stressed Silicone Rubber/Silica Micro and Nanocomposite for the Coating High Voltage Insulation Applications, *Mater.*, 2021, **14**(13), DOI: **10.3390/ma14133567**.

12 I. Ramirez, R. Hernandez and G. Montoya, Salt fog testing of RTV coated ceramic insulators and comparison with HTV silicone rubber insulators, in *2012 Annual Report Conference on Electrical Insulation and Dielectric Phenomena*, 14–17 Oct. 2012, 2012, pp. 794–797, DOI: **10.1109/CEIDP.2012.6378900**.

13 P. Ashitha, S. Akhil, L. Gaurav and K. Meena, Influence of non ionic surfactant on electrical and hydrophobic properties of binary composites of silicone rubber, *Mater. Today: Proc.*, 2021, **44**, 2421–2424.

14 S. Kashi, *et al.*, Mechanical, Thermal, and Morphological Behavior of Silicone Rubber during Accelerated Aging, *Polym.-Plast. Technol. Eng.*, 2018, **57**, 1–10, DOI: **10.1080/03602559.2017.1419487**.

15 B. Venkatesulu and M. J. Thomas, Long-term accelerated weathering of outdoor silicone rubber insulators, *IEEE Trans. Dielectr. Electr. Insul.*, 2011, **18**(2), 418–424, DOI: **10.1109/TDEI.2011.5739445**.

16 E. A. Cherney, Silicone rubber dielectrics modified by inorganic fillers for outdoor high voltage insulation applications, *IEEE Trans. Dielectr. Electr. Insul.*, 2005, **12**(6), 1108–1115.

17 A. Farahani, M. Jamshidi and M. Foroutan, Improving thermal/electrical properties of silicone rubber nanocomposite using exfoliated boron nitride nano sheets made by an effective/novel exfoliating agent, *Mater. Des.*, 2023, **229**, 111935, DOI: **10.1016/j.matdes.2023.111935**.

18 K. Zaffer and P. Sammaiah, Improvement of Electrical Insulation in Silicone Rubber by Adding Al$_2$O$_3$, *Int. J. Innov. Technol. Explor. Eng.*, 2019, **8**(10), 4695–4698.

19 A. H. El-Hag, S. H. Jayaram and E. A. Cherney, Comparison between silicone rubber containing micro- and nano- size silica fillers [insulating material applications], in *The 17th Annual Meeting of the IEEE Lasers and Electro-Optics Society, 2004. LEOS 2004*, 20–20 Oct. 2004, 2004, pp. 385–388, DOI: **10.1109/CEIDP.2004.1364268**.

20 S. Fang, Z. Jia, H. Gao and Z. Guan, Influence of fillers on silicone rubber for outdoor insulation, in *2007 Annual Report - Conference on Electrical Insulation and Dielectric Phenomena*, 14-17 Oct. 2007, 2007, pp. 300-303, DOI: **10.1109/CEIDP.2007.4451459**.

21 F. Deeba, K. Shrivastava, M. Bafna and A. Jain, Tuning of Dielectric Properties of Polymers by Composite Formation: The Effect of Inorganic Fillers Addition, *J. Compos. Sci.*, 2022, **6**(12), 355.

22 A. Khattak, A. U. Rehman, A. Ali, A. Mahmood, K. Imran, A. Ulasyar, H. Sheh Zad, N. Ullah and A. Khan, Multi-stressed nano and micro-silica/silicone rubber composites with improved dielectric and high-voltage insulation properties, *Polymers*, 2021, **13**(9), 1400, DOI: **10.3390/polym13091400**.

23 H. Khan, A. Mahmood, I. Ullah, M. Amin and M. T. Nazir, Hydrophobic, dielectric and water immersion performance of 9000 h multi-stresses aged silicone rubber composites for high voltage outdoor insulation, *Eng. Failure Anal.*, 2021, **122**, 105223.

24 H. M. Schneider, W. W. Guidi, J. T. Burnham, R. S. Gorur and J. F. Hall, Accelerated aging and flashover tests on 138 kV nonceramic line post insulators, *IEEE Trans. Power Delivery*, 1993, **8**(1), 325–336, DOI: **10.1109/61.180353**.

25 I. Standard, 60093, Methods of Test for Volume Resistivity and Surface Resistivity of Solid Electrical Insulating Materials, International Electrotechnical Commission, 1980.

26 I. E. Commission, Recommended methods for the determination of the permittivity and dielectric dissipation factor of electrical insulating materials at power, audio and radio frequencies including metre wavelengths, IEC Standard 60250: 1969, 1969.

27 A. Zolriasatein, S. Navazani, M. R. Abadchi and N. R. Noori, Two-component room temperature vulcanized silicone-rubber (RTV2) properties modification: Effect of aluminum three hydrate and nanosilica additions on the microstructure, electrical, and mechanical properties, *J. Mater. Sci.: Mater. Electron.*, 2021, **32**, 8903–8915.

28 C. International Electrotechnical, Medical electrical equipment-Part 1: General requirements for basic safety and essential performance, IEC 60601-1: 2005, 2005, 2005. [Online]. Available: **https://cir.nii.ac.jp/crid/1570572701237862400**.

29 P. Barber, *et al.*, Polymer Composite and Nanocomposite Dielectric Materials for Pulse Power Energy Storage, *Materials*, 2009, **2**(4), 1697–1733, DOI: **10.3390/ma2041697**.

30 L. K. Namitha and M. T. Sebastian, Microwave dielectric properties of flexible silicone rubber – Ba(Zn1/3Ta2/3)O3 composite substrates, *Mater. Res. Bull.*, 2013, **48**(11), 4911–4916, DOI: **10.1016/j.materresbull.2013.07.029**.

31 Z. Farhadinejad, M. Ehsani, I. Ahmadi-Joneidi, A. A. Shayegani and H. Mohseni, Effects of UVC radiation on thermal, electrical and morphological behavior of silicone rubber insulators, *IEEE Trans. Dielectr. Electr. Insul.*, 2012, **19**(5), 1740–1749, DOI: **10.1109/TDEI.2012.6311523**.

32 I. A. Joneidi, A. A. Shayegani and H. Mohseni, Influence of ultra violet radiation on the surface and leakage current of silicone rubber insulator, *Int. J. Phys. Sci.*, 2011, **6**(22), 5109–5120.

33 A. Syakur, *et al.*, A Study of Leakage Current Characteristic of Silicone Rubber Surface after Subjected to Ultraviolet Light, in *2021 International Conference on Smart-Green Technology in Electrical and Information Systems (ICSGTEIS)*, 28–30 Oct. 2021, 2021, 142–145, DOI: **10.1109/ICSGTEIS53426.2021.9650372**.